

File ID 355808
Filename Chapter 8: Concluding remarks and outlook

SOURCE (OR PART OF THE FOLLOWING SOURCE):

Type Dissertation
Title Quantitative and localized spectroscopy for non-invasive bilirubinometry in neonates
Author N. Bosschaart
Faculty Faculty of Medicine
Year 2012
Pages 108
ISBN 978-94-6182-065-5

FULL BIBLIOGRAPHIC DETAILS:

<http://dare.uva.nl/record/410666>

Copyright

It is not permitted to download or to forward/distribute the text or part of it without the consent of the author(s) and/or copyright holder(s), other than for strictly personal, individual use.

CHAPTER 8

Concluding remarks and outlook

This Chapter reflects on the content of this thesis. The current status of LCS as a technique for non-invasive bilirubinometry is discussed and possibilities for further improvement of the technique are addressed. Since the application of LCS is not restricted to bilirubinometry on neonates, we also describe other potential applications for this new technique.

8.1 Introduction

In Chapters 1 and 2, the limitations of currently used optical techniques for transcutaneous bilirubinometry were introduced: whereas transcutaneous bilirubinometers are suited as a screening method for hyperbilirubinemia, these devices cannot serve as a replacement of invasive blood sampling. The major reason for this is the fact that these devices measure the extravascular bilirubin concentration, which cannot be directly related to the parameter of interest: the intravascular, or total serum bilirubin concentration (TSB). We suggested two approaches to solve this problem, from both a medical and a technological perspective. This thesis focused on the technological approach, by designing a spectroscopic technique (low-coherence spectroscopy, LCS) that can confine its probing volume to the intravascular space only. Thereby, a one to one comparison between the spectroscopic bilirubin measurement and the TSB can be achieved. Hence, LCS may become the technique that can completely replace invasive blood sampling for TSB determination, leading to less pain, stress and a faster diagnosis for jaundiced neonates.

Since LCS is a new technique, this thesis describes the essential first steps in the design, development and validation of the technique (Chapters 4 and 5). The measured attenuation coefficients ($0.15 - 34 \text{ mm}^{-1}$) by LCS on tissue simulating phantoms are within the range of the neonatal skin optical properties described in Chapter 3 ($\mu_t = \mu_a + \mu_s'/(1-g) \approx 10 - 20 \text{ mm}^{-1}$ when a scattering anisotropy of $g = 0.85$ is assumed [1]). In addition to the phantom experiments, we proved that we can use LCS to measure local absorption coefficient spectra in real, living tissue and that biologically relevant chromophore concentrations could be obtained from the measured absorption spectra (Chapter 6). To further improve the acquisition speed and sensitivity of the technique, Chapter 7 presented a new method for spectroscopic detection in LCS. Hence, we demonstrated that LCS is a very promising technique for non-invasive bilirubin measurements.

Before LCS can be clinically applied, further research is needed on 1) the applicability of LCS for measuring the μ_t in whole blood, 2) the quantification of bilirubin concentrations from the measured μ_t of whole blood and 3) improvements on the speed, sensitivity and design of our current LCS system. Sections 8.2 and 8.3 of this Chapter discuss these issues in detail. Since the application of LCS is not restricted to bilirubinometry, Section 8.4 discusses other potential applications for this new technique.

8.2 *In vivo* LCS measurements of whole blood

As described in Chapters 1 and 2, and Section 8.1, we intend to use LCS for measuring the absorption coefficient spectrum within a single blood vessel. From the measured spectrum, we want to obtain the bilirubin concentration in whole blood, comparable to our method of obtaining the hemoglobin concentration in Chapter 6.2.2. Naturally, this raises the question: is LCS sensitive enough to measure the high attenuation associated with the large absorption and scattering in whole blood?

Based on the measured SNR of our tdLCS system (~ 50 dB, Figure 7.5), we should be able to measure optical densities ($\text{OD} = \mu_t \cdot \ell$) of maximally $\ln(10^5) = 11.5$. The epidermal OD measured in Chapter 6 was approximately 0.8. Hence, if we measure inside a blood vessel located beneath the epidermis, the remaining maximal OD for our measurement is $11.5 - 0.8 = 10.7$. If we assume a diameter of 0.1 mm ($\ell = 0.2$ mm) for this blood vessel, the maximal attenuation coefficient that LCS can measure over the full diameter of this vessel is $\mu_t = 10.7/0.2 = 53.5 \text{ mm}^{-1}$.

Around the center wavelength of our LCS system, whole blood has an absorption coefficient of $\sim 30 \text{ mm}^{-1}$ and a scattering coefficient of $\sim 300 \text{ mm}^{-1}$ [2], resulting in a total attenuation coefficient of $\mu_t \approx 330 \text{ mm}^{-1}$. This μ_t for whole blood is larger than the maximal attenuation coefficient that LCS can measure. However, when measuring on such a highly scattering medium with large anisotropy ($g = 0.99$) [2], multiple scattering contributions to the LCS signal are inevitable. As was discussed in Chapter 5, these contributions can lower the effective μ_s -contribution to the μ_t that is measured by LCS, while the μ_a -contribution remains unaffected, since absorption takes place along the photon's path (Chapter 4). Although we do not know the exact influence of these and other effects on LCS measurements on whole blood, we will show an experimental validation of the performance of LCS on whole blood in the next section.

8.2.1 Experimental validation

To validate the performance of LCS in whole blood, we performed an *in vivo* tdLCS measurement on the nail and the underlying nail bed of the index finger of a healthy human volunteer. The measurement settings and method of analysis were identical to the methods described in Chapter 6.2. Figure 8.1 shows the resulting OCT image, with three dark regions in the nail bed, which are presumably blood vessels. A region of interest within one of the presumed blood vessels was selected (dashed rectangle: $200 \times 110 \mu\text{m}^2$, width \times depth) for the determination of μ_t . The measured attenuation coefficient spectrum (dots) within this region was fitted with a μ_t -fit (solid line) as described in Chapter 6.2.2, assuming the presence of oxygenized and deoxygenized hemoglobin in the vessel. The OD of the tissue covering the blood vessel was approximately 0.75.

The highest measured μ_t -values within the vessel (57 mm^{-1}) are close to the predicted maximal measurable value of 53.5 mm^{-1} . The μ_s -contribution to the μ_t -fit ($\sim 5 \text{ mm}^{-1}$) is low compared to the expected μ_s for whole blood, which may be explained by the contribution of multiple scattering to the LCS signal. Strikingly, the measured and fitted values of μ_t are very similar to the absorption coefficient of whole blood [2]. In fact, the fitted total hemoglobin concentration ([tHb]) was $143 \pm 24 \text{ g/L}$, which is within the physiological [tHb] range of 134 to 173 g/L for whole blood [2]. In addition, the fitted oxygen saturation (SO_2) of $60 \pm 29 \%$ resembled the SO_2 of venous blood [3].

These results show that *in vivo* LCS measurements on whole blood within a blood vessel are possible. Although the current accuracy of the measurement is too low for clinical applications, this accuracy is likely to be improved when the configuration for sdLCS is optimized (Chapter 7 and Section 8.3.1).

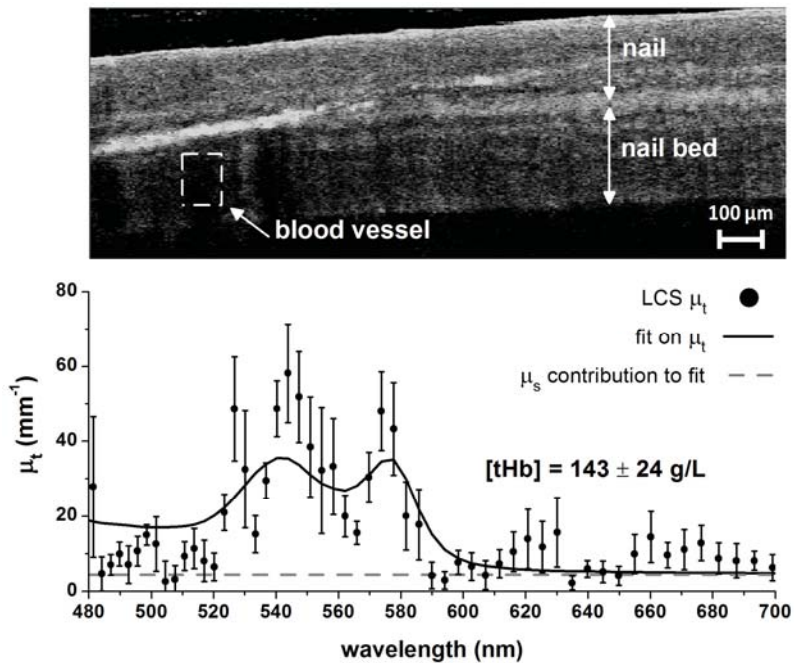


Figure 8.1 In vivo LCS measurement on a blood vessel under the nail of an index finger. The upper OCT image shows the nail, the nail bed and the selected blood vessel region for the determination of μ_t (dashed rectangle). The lower graph shows the attenuation spectrum within the selected region, the fit on μ_t and the μ_s -contribution to the μ_t -fit. The fitted total hemoglobin concentration $[tHb]$ (143 ± 24 g/L) is within the physiological $[tHb]$ range of 134 to 173 g/L for whole blood.

8.2.2 Blood flow influences on the LCS signal

Blood flow induces Doppler shifting of the modulation frequency of the LCS signal. This has different consequences for tdLCS and sdLCS. Since the frequency shifted signals are remapped to a wavelength axis in tdLCS, Doppler shifting by blood flow induces a translation of the LCS spectrum along the wavelength axis, comparable to the spectral broadening by Brownian motion (Chapter 4). This may not only induce an error in the determination of the optical coefficients, it may also lead to a complete loss of signal if the frequency shift extends the bounds of the lock-in filter. Although we did not encounter any influences of blood flow induced Doppler shifting in the measurements presented in Chapter 6 and Section 8.2.1, the influences of blood flow should not be overlooked when using tdLCS. To avoid Doppler shifting of the LCS signal, the angle of incidence on the blood vessel can be set to 90 degrees. Since this may be difficult to realize in practice, a temporary stop of blood flow can be realized during the measurement by a (manual) occlusion of the vessel.

For sdLCS, Doppler shifting by blood flow has less influence on the measured spectrum compared to tdLCS. Since a Doppler frequency shift will be negligible compared to the frequency of light, a translation of the measured spectrum along the wavelength axis will not occur. However, a Doppler frequency shift extending the bounds of the frequency domain filter (Figure 7.1f) can induce loss of signal. The latter

may be avoided by a careful choice of the modulation frequency and filter bounds, a 90 degree angle of incidence or temporary occlusion of the vessel. Another effect of blood flow on the sdLCS signal may be a decrease of the modulation depth in $i_D(\lambda)$ ('fringe wash-out', see Chapter 7.7), since the scattering red blood cells move during the integration time of the spectrograph. This problem may be solved by faster acquisition (Section 8.3.1).

8.2.3 Bilirubin concentration measurements by LCS

The *in vivo* LCS measurements described in Chapter 6 and Section 8.2.1 focused on the measurement of oxygenized and deoxygenized hemoglobin concentrations. Although this does not directly demonstrate the capability of LCS to measure bilirubin concentrations, it proves the capability of the technique to derive biologically relevant tissue chromophore concentrations from an attenuation coefficient spectrum. The bilirubin absorption peak around 460 nm (Figure 1.1) falls just outside the spectral range of our LCS measurements, because of the decrease in SNR in this region (Figure 7.5). Although the SNR around 460 nm of the sdLCS system shows an improvement with respect to tdLCS, further improvements in LCS system design may be needed for accurate bilirubin concentration measurements (Section 8.3.1).

For the clinical assessment of whole blood bilirubin concentrations in neonates, an accuracy of at least 10 $\mu\text{mol/L}$ within the range of 40 to 400 $\mu\text{mol/L}$ is desired, which translates into an accuracy of 0.13 mm^{-1} for the determination of μ_a . Although the current accuracy in μ_a of 0.5 mm^{-1} is close to this required value (Chapter 4), further improvements on LCS accuracy are needed (Section 8.3.1). Nevertheless, with the current accuracy in μ_a we would be able to measure bilirubin concentration changes of 40 $\mu\text{mol/L}$, which is comparable to the accuracy of existing transcutaneous bilirubinometers [4]. Hence, further research on LCS for non-invasive bilirubinometry is justified.

In contrast to the existing bilirubinometers, LCS can potentially be applied for continuous monitoring of bilirubin levels, which may provide more insight into bilirubin physiology and reduces the time for treatment decision making. Existing devices cannot be used for this purpose, because photo bleaching of bilirubin decreases the bilirubin concentration in the extravascular space [5], introducing an additional measurement error. Since LCS will be applied for bilirubin concentration measurements on flowing blood in the intravascular space, the effect of photo bleaching will be negligible.

8.3 Possibilities for LCS system improvement

8.3.1 Speed and sensitivity

As mentioned in Chapter 7 and Section 8.2, the speed and sensitivity of the current LCS system need to be improved. In Section 7.2.2, we showed that spectroscopic detection with sdLCS induces a theoretical sensitivity advantage compared to tdLCS. Furthermore, a trade-off exists between the speed and sensitivity of an LCS system, since acquisition speed can be enhanced by sacrificing sensitivity.

Since the quantum efficiency and acquisition speed of the USB4000 spectrograph, used for spectral detection, are not optimized for sdLCS, we could not demonstrate a

sensitivity advantage compared to tdLCS in Chapter 7. However, we did demonstrate that our method for spectroscopic detection in LCS is feasible. Therefore, the most straightforward method to realize a speed and sensitivity enhancement in LCS, is by implementing a spectrograph that is optimized for sdLCS. The maximal sensitivity advantage that can be achieved with an sdLCS system will depend on the number of pixels, the quantum efficiency, and the ΔL_{\max} of the spectrograph (Eq. 7.10). Hence, these parameters should be considered when optimizing the sdLCS system, as well as the trade-off between acquisition speed and sensitivity. In addition, sensitivity may be improved by (lateral) averaging of spectra, which increases the SNR with the square root of the number of averages.

As demonstrated in Chapter 7.7, a spectrograph with 17 kHz acquisition rate (100 times faster than the USB4000) matches the acquisition speed requirements for sdLCS. With this acquisition rate, the determination of the attenuation spectrum in the blood vessel of Section 8.2.1 would only take 12 ms. Since 140 kHz line rate cameras with high quantum efficiency are available [6], such an sdLCS system is realizable.

For the purpose of bilirubinometry, it may be advantageous to enhance the sensitivity of the sdLCS system for wavelengths around 460 nm (Section 8.2.3). The current SNR in this wavelength band is relatively low due to a combination of detector quantum efficiency and source power. Detector quantum efficiency around 460 nm can be enhanced by choosing a detector that is optimized for this wavelength range, e.g. visible/UV-enhanced detectors that have a considerably higher quantum efficiency compared to regular silicon based detectors below 500 nm [7,8]. Recently, supercontinuum sources became available with higher output power around 460 nm compared to the source in our LCS system [9]. Furthermore, collimated broad band LED's are available with high output power around the bilirubin absorption peak [10]. However, since these LED's do not have a single mode output spectrum, the effects of modal dispersion and intermodal interference need to be reevaluated when implementing these sources in our LCS system.

8.3.2 Compactness and clinical utility

Before LCS can be introduced into the clinic, several adjustments to the current bench-top system design are necessary. To reduce the size of the system, the open air optical paths can be replaced by fiber optic paths. In addition, the development of a fiber based probe in the sample arm will be necessary to facilitate clinical measurements. A fiber based LCS system requires careful design and choice of optical components, since a large wavelength bandwidth needs to be guided through single mode and/or multimode fibers while avoiding signal loss and the effects of modal dispersion and intermodal interference. Recent advances in the field of integrated optics have lead to e.g. chip-based spectrographs [11]. Therefore, further reduction of the LCS system size may be achieved by integrating several or more system components on a chip.

As was demonstrated in Chapter 6, lateral scanning of the sample is needed for spatial averaging of the LCS signal. The current implementation for lateral sample scanning involves movement of the sample with respect to the sample arm beam. For clinical purposes, it will be advantageous to scan the sample arm beam with respect to the sample. This can be achieved by implementing x/y-lateral scanning mirrors, as is

commonly done in clinical OCT systems [12]. The implementation of x/y-lateral scanning introduces the additional possibility to make a volume scan of the sample, instead of a single B-scan as in Figure 8.1, which facilitates the localization of blood vessels (Section 8.3.3). Also the current method for axial scanning of the sample, involving movement of the sample with respect to the sample lens, needs to be replaced by translation of the sample lens with respect to the sample. The latter will require an adjustment of the focus tracking scheme described in Chapter 4.

8.3.3 Blood vessel localization

In Chapter 6 and Section 8.2.1, the localization of the region of interest for the determination of μ_t was supported by an OCT image that was reconstructed from the LCS signal. Since only the spectral information within the region of interest is required, the relatively slow step-wise LCS scanning outside the region of interest may be replaced by other imaging modalities for blood vessel localization. Possible imaging modalities for this purpose are conventional OCT imaging, photoacoustic tomography [13] and side stream dark field (SDF) imaging [14]. Naturally, this requires precise coalignment of these modalities with the LCS signal. Although such a design has consequences for the compactness of the system, it is likely to result in a considerably faster localization of blood vessels that are suited for LCS μ_t -determination.

8.4 Other potential applications of LCS

Besides its value for non-invasive bilirubin measurements, LCS creates new opportunities within and outside the field of tissue spectroscopy. Supported by the structural tissue information of an OCT image, LCS offers the possibility to accurately and simultaneously quantify a unique set optical property spectra (μ_t , μ_a , μ_s and μ_b) and tissue chromophore concentrations within a very confined and controllable tissue volume of choice. No other spectroscopic technique is capable of doing such a determination. As a consequence, LCS solves many methodological problems related to conventional reflectance spectroscopy, e.g. assumptions on photon path lengths, probing volume and homogeneity of the investigated tissue. This offers new opportunities for tissue diagnostic applications.

Recent advances in the field of spectroscopic optical coherence tomography (sOCT), which is closely related to LCS (Chapter 4.1), further emphasize the need for techniques like LCS by showing progression in localized measurements of optical properties [15]. Since the focus of this research is on OCT image contrast enhancement, the quantification and localization of chromophore concentrations and attenuation spectra is not as accurate and well-validated as in LCS. Nevertheless, the research area of LCS and LCS-related research is becoming increasingly important in the field of tissue optics. This section describes other potential applications for LCS.

8.4.1 Applications based on absorption

In Chapter 6 and Section 8.2, we showed that LCS can be used for the determination of other chromophore concentrations than bilirubin. By measuring hemoglobin absorption spectra, not only the total hemoglobin concentration could be determined,

but also the oxygen saturation within the investigated tissue volume. Accurate determination of total hemoglobin concentrations and oxygen saturation within blood vessels can potentially replace the need for this determination by invasive blood sampling in both neonates and adults. In addition, knowledge of the hemoglobin concentration and oxygen saturation within confined tissue volumes consisting of both intravascular and extravascular tissue space can provide valuable information on tissue physiology and pathology, e.g. during shock.

The current LCS system was optimized for the visible wavelength range. As a consequence, only concentrations of chromophores with distinct absorption features within this wavelength region could be quantified. However, LCS is not limited to the visible range and may be extended to the ultraviolet and (near) infrared region for the quantification of e.g. water concentration (related to skin hydration) and potentially glucose concentration (for the monitoring of diabetic patients). Also the delivery and distribution of exogenous therapeutic and contrast agents with distinct absorption, or scattering features may be monitored by LCS.

8.4.2 Applications based on scattering

Chapter 5 demonstrated that LCS is not only a promising technique for the determination of local absorption coefficient spectra, but also for the determination of local scattering, and backscattering coefficient spectra. Based on this determination, we showed that LCS can be used for the characterization of samples, in terms of particle size and concentration. This may be an interesting application within the field of particle science. Furthermore, the quantitative and wavelength dependent measurement of μ_s and μ_b makes the technique sensitive for changes in cell morphology and organization, which may be relevant for (early) cancer detection and monitoring of tumor development [16]. The additional absorption coefficient based information on hemoglobin concentration and oxygen saturation, related to tumor vascularization [17], results in an extensive and unique set of 'tumor sensitive' parameters that can only be measured simultaneously by LCS. Hence, also the application of cancer diagnosis by LCS deserves further investigation.

In addition to the quantitative measurement of optical coefficients, LCS can also be used for deriving path length resolved blood flow, or perfusion related parameters from the back scattered signal. These parameters can be quantified by measuring the blood-flow related speckle decorrelation rate of the LCS signal, or the Doppler frequency shift (see also Section 8.2.2), as has been demonstrated before with other low-coherence interferometry based modalities [18,19].

8.5 Concluding remarks

Summarizing, this thesis described the essential first steps in the design, development and validation of LCS as a method for the quantitative and localized determination of tissue optical properties and chromophore concentrations. As an outlook, following the suggested steps on improving the speed and sensitivity of the technique is required before LCS can be introduced into the clinic for the purpose of non-invasive bilirubinometry and other potential applications. Nevertheless, even with the sub-

optimal sensitivity of the current time domain LCS system, we can already show that LCS can be used for measuring the μ_a within a single blood vessel in human skin, and that the derived hemoglobin concentration is well within the range of normal human whole blood hemoglobin concentrations. Therefore, LCS is a very promising technique that deserves further development and can potentially lead to less pain and complications for preterm neonates.

References

1. M.J.C. van Gemert, S.L. Jacques, H.J.C.M. Sterenborg, W.M. Star, "Skin Optics", *IEEE Transactions on Biomedical Engineering* **36**, 1146-1154 (1989)
2. A. Roggan, M. Friebel, K. Dörschel, A. Hahn, G. Müller, "Optical properties of circulating human blood in the wavelength range 400-2500 nm", *Journal of Biomedical Optics* **4**, 36-46 (1999)
3. A. Keys, "The oxygen saturation of the venous blood in normal human subjects", *American Journal of Physiology*, 13-21 (1938)
4. K. Grohmann, M. Roser, B. Rolinski, I. Kadow, C. Muller, A. Goerlach-Graw, M. Nauck, H. Kuster, "Bilirubin measurement for neonates: comparison of 9 frequently used methods", *Pediatrics* **117**, 1174-1183 (2006)
5. G. Agati, F. Fusi, G.P. Donzelli, R. Pratesi, "Quantum yield and skin filtering effects on the formation rate of lumirubin", *Journal of Photochemistry and Photobiology B: Biology* **18**, 197-203 (1993)
6. Basler Sprint line scan camera: www.baslerweb.com
7. Princeton Instruments CCD camera's: www.princetoninstruments.com
8. Andor Technology CCD camera's: www.andor.com
9. Fianium supercontinuum sources: www.fianium.com
10. Thorlabs collimated LED sources: www.thorlabs.de
11. V.D. Nguyen, B.I. Akca, K. Worhoff, R.M. de Ridder, M. Pollnau, T.G. van Leeuwen, J. Kalkman, "Spectral domain optical coherence tomography imaging with an integrated optics spectrometer", *Optics Letters* **36**, 1293-1295 (2011)
12. E.A. Swanson, J.A. Izatt, M.R. Hee, D. Huang, C.P. Lin, J.S. Schuman, C.A. Puliafito, J.G. Fujimoto, "In vivo retinal imaging by optical coherence tomography", *Optics Letters* **18**, 1864-1866 (1993)
13. L.V. Wang, "Multiscale photoacoustic microscopy and computed tomography", *Nature Photonics* **3**, 503-509 (2009)
14. P.T. Goedhart, M. Khalilzada, R. Bezemer, J. Merza, C. Ince, "Sidestream dark field (SDF) imaging: a novel stroboscopic LED ring-based imaging modality for clinical assessment of the microcirculation", *Optics Express* **15**, 15101-15114 (2007)
15. F.E. Robles, C. Wilson, G. Grant, A. Wax, "Molecular imaging true-colour spectroscopic optical coherence tomography", *Nature Photonics*, doi:10.1038/nphoton.2011.257 (2011)
16. H. Subramanian, H.K. Roy, P. Pradhan, M.J. Goldberg, J. Muldoon, R.E. Brand, C. Sturgis, T. Hensing, D. Ray, A. Bogojevic, J. Mohammed, J. Chang, V. Backman, "Nanoscale cellular changes in field carcinogenesis detected by partial wave spectroscopy", *Cancer Research* **69**, 5357-5363 (2009)
17. P. Vaupel, F. Kallinowski, P. Okunieff, "Blood flow, oxygen and nutrient supply, and metabolic microenvironment of human tumors: a review", *Cancer Research* **49**, 6449-6465 (1989)
18. J. Kalkman, R. Sprik, T.G. van Leeuwen, "Path-length-resolved diffusive particle dynamics in spectral domain optical coherence tomography", *Physical Review Letters* **105**, 198302 (2010)
19. B. Varghese, V. Rajan, T.G. van Leeuwen, W. Steenbergen, "Path-length-resolved optical Doppler perfusion monitoring", *Journal of Biomedical Optics* **12**, 060508 (2007)